An investigation of valence shell orbital momentum profiles of difluoromethane by binary $(e,2e)$ spectroscopy

G. L. Su, C. G. Ning, S. F. Zhang, X. G. Ren, H. Zhou, B. Li, F. Huang, G. Q. Li, and J. K. Deng[a)]
Department of Physics, Tsinghua University, Beijing 100084, People's Republic of China

(Received 7 September 2004; accepted 4 November 2004; published online 13 January 2005)

The electron binding energy spectra and momentum profiles of the valence orbitals of difluoromethane, also known as HFC32 (HFC—hydrofluorocarbon) (CH_2F_2), have been studied by using a high resolution $(e,2e)$ electron momentum spectrometer, at an impact energy of 1200 eV plus the binding energy, and by using symmetric noncoplanar kinematics. The experimental momentum profiles of the outer valence orbitals and $4a_1$ inner valence orbital are compared with the theoretical momentum distributions calculated using Hartree–Fock and density functional theory (DFT) methods with various basis sets. In general, the shapes of the experimental momentum distributions are well described by both the Hartree–Fock and DFT calculations when large and diffuse basis sets are used. However, the result also shows that it is hard to choose the different calculations for some orbitals, including the methods and the size of the basis sets employed. The pole strength of the ionization peak from the $4a_1$ inner valence orbital is estimated. © *2005 American Institute of Physics.* [DOI: 10.1063/1.1839851]

I. INTRODUCTION

Electron momentum spectroscopy (EMS) has been used extensively for the investigation of molecular electronic structure due to its unique ability to measure the momentum profiles for individual molecular orbitals. Within the plane wave impulse approximation (PWIA) and the target Hartree–Fock approximation (THFA) or target Kohn–Sham approximation (TKSA), the measured $(e,2e)$ cross section is proportional to the spherically averaged momentum distribution of a specific molecular orbital. Therefore, EMS is usually taken as a powerful technique for evaluating the quality of quantum chemical calculations.[1–3]

EMS has been successfully applied to an increasingly wide variety of atomic, molecular, and solid-state targets and has long been shown to provide stringent tests for Hartree–Fock (HF) level and correlated configuration interaction (CI) molecular wave functions.[1,3–6] More recently EMS has provided an effective test for the evaluation of Kohn–Sham density functional theory (DFT) (Ref. 7) for a range of small and larger molecules.[5,6,8–12] It has been shown by a large number of EMS measurements on various targets that inclusion of electron correlation in theoretical calculations (e.g., CI or DFT methods) will reproduce the experimental momentum distribution better.[4–6,8–12] It is interesting to note that recently Neerja, Tripathi, and Smith[13] evaluated experimental momentum density using wave functions at different levels of correlation together with density functional methods and showed that the momentum distributions are sensitive to the correlation effect, especially in the lower-momentum region.

As EMS studies progressed to larger molecules, sufficiently accurate CI calculations became more difficult to perform. However, the recent work by Duffy *et al.*[4,8] and Casida[14] shows that the DFT method using the exchange-correlation functionals provides as close a match to the experimental data as CI calculations do. So DFT will be a natural choice for large systems at the present level.

On the other hand, it should also be noted that EMS is particularly sensitive to the low momentum part of the frontier orbital densities that may be important in molecular recognition and the initial processes involved in the early stages of a chemical reaction. Cooper *et al.*[15] have shown that the assessment of electron density topographies is much more effectively carried out in momentum space than in the more commonly used position space.

Difluoromethane, also known as HFC32 (HFC—hydrofluorocarbon) (CH_2F_2), is an important refrigerating medium and fire extinguishing agent. Now it is called a green refrigerating medium because it does not damage the ozone layer and does not have the potential contribution to global warming.[16] Furthermore, it has become a chlorofluorocarbon replacement of HFC in industrial applications.[17] Detailed knowledge of the electronic structure of difluoromethane is of great importance due to their wide usage in industry and their large potentials for atmospheric ozone in the stratosphere.[16] Difluoromethane has been widely studied not only by He I and He II photoelectron spectroscopy (PES)[18,19] and x-ray photoelectron spectroscopy,[20] but also by the theoretical works.[21] The measured results of the binding energy spectra from 7–32 eV at $\varphi=1°$ and 10° angles and the momentum distributions of the highest occupied molecular orbital (HOMO) $2b_1$ of CH_2F_2 have been recently reported.[22] In this paper, the valence binding energy spectra at the sum of all the φ angles and electron momentum profiles for the outer valence orbitals and $4a_1$ inner valence

[a)]Author to whom correspondence should be addressed. Department of Physics, Tsinghua University, Beijing 100084, People's Republic of China. Electronic mail: djk-dmp@mail.tsinghua.edu.cn

TABLE I. Basis sets and calculated properties for difluoromethane.

Methods	Basis set [C,F]/[H]	Total energy (a.u.)	Dipole moment (D)
HF/STO-3G	Gaussian $[2s1p]/[1s]$	−234.625	1.298
HF/6-31G	Gaussian $[3s2p]/[2s]$	−237.823	2.758
HF/6-311++G**	Gaussian $[5s4p1d]/[4s1p]$	−237.904	2.500
HF/aug-cc-pVTZ	Gaussian $(10s,5p,2d,1f)/[4s,3p,2d,1f]$	−237.999	2.270
B3LYP/6-31G	Gaussian $[3s2p]/[2s]$	−238.919	2.207
B3LYP/6-311++G**	Gaussian $[5s4p1d]/[4s1p]$	−239.068	2.201
B3LYP/aug-cc-pVTZ	Gaussian $(10s,5p,2d,1f)/[4s,3p,2d,1f]$	−239.091	2.010
Experimental[a]			1.970

[a]Reference 23.

orbital of CH_2F_2 have been measured using an energy dispersive multichannel $(e,2e)$ electron momentum spectrometer at an impact energy of 1200 eV plus binding energy and in a symmetric noncoplanar geometry. The experimental momentum profiles are also compared with HF and DFT calculations using various basis sets.

II. THEORETICAL BACKGROUND

In a binary $(e,2e)$ experiment, the scattered and the ionized electrons are detected at the same kinetic energies and the same polar angles in symmetric noncoplanar scattering geometry. Under conditions of high impact energy and high momentum transfer, the target electron essentially undergoes a clean ''knock-out'' collision and the PWIA provides a very good description of the collision. In the PWIA, the momentum p of the electron prior to knockout is related to the azimuthal angle by[1]

$$p=\{(2p_1\cos\theta_1-p_0)^2+[2p_1\sin\theta_1\sin(\phi/2)]^2\}^{1/2}, \tag{1}$$

where $p_1=p_2=\sqrt{2E_1}$ is the magnitude of the momentum of each outgoing electron and $p_0=\sqrt{2E_0}$ is the momentum of the incident electron (both in atomic units). Under these conditions the kinematic factors are effectively constant,[1] the EMS cross section for randomly oriented gas-phase targets σ_{EMS} can be given by

$$\sigma_{\mathrm{EMS}}\propto S_f^2\int d\Omega|\langle\mathbf{p}\Psi_f^{N-1}|\Psi_i^N\rangle|^2, \tag{2}$$

where $\mathbf{p}$ is the momentum of the target electron prior to ionization and S_f^2 is pole strength. $|\Psi_f^{N-1}\rangle$ and $|\Psi_i^N\rangle$ are the total electronic wave functions for the final ion state and the target molecule ground (initial) state, respectively. The $\int d\Omega$ represents the spherical average due to the randomly oriented gas-phase target. The overlap of the ion and neutral wave functions in Eq. (2) is known as the Dyson orbital while the square of this quantity is referred to as an ion-neutral overlap distribution. Thus, the $(e,2e)$ cross section is essentially proportional to the spherical average of the square of the Dyson orbital in momentum space.

Equation (2) is greatly simplified by using the THFA. Within the THFA, only final (ion) state correlation is allowed and the many-body wave functions $|\Psi_f^{N-1}\rangle$ and $|\Psi_f^N\rangle$ are approximated as independent particle determinants of ground state target Hartree–Fock orbitals. In this approximation Eq. (2) reduces to

$$\sigma_{\mathrm{EMS}}\propto S_j^f\int d\Omega|\psi_j(p)|^2, \tag{3}$$

where $\psi_j(p)$ is the one-electron momentum space canonical Hartree–Fock orbital wave function for the jth electron, corresponding to the orbital from which the electron was ionized, S_j^f is the spectroscopic factor, the probability of the ionization event producing a one-hole configuration of the final ion state. The integral in Eq. (3) is known as the spherically averaged one-electron momentum distribution. To this extent EMS has the ability to image the electron density in individual ''orbitals'' selected according to their binding energies.

Equation (2) has recently been reinterpreted[7] in the context of Kohn–Sham DFT and the TKSA gives a result similar to Eq. (3) but with the canonical Hartree–Fock orbital replaced by a momentum space Kohn–Sham orbital $\psi_j^{\mathrm{KS}}(p)$,

$$\sigma_{\mathrm{EMS}}\propto\int d\Omega|\psi_j^{\mathrm{KS}}(\mathbf{p})|^2. \tag{4}$$

It should be noted that accounting of electron correlation effects in the target ground state is included in the TKSA via the exchange-correlation potential. A more detailed description of the TKSA-DFT method may be found elsewhere.[7]

In the present work, spherically averaged theoretical momentum profiles have been calculated for the outer valence orbitals and $4a_1$ inner valence orbital of CH_2F_2 using the PWIA. The calculation methods and basis sets are described briefly below and in Table I. The total number of contracted Gaussian-type orbital functions (CGTO) is also given for each calculation below. The total energies and the dipole moments of CH_2F_2 predicted by these various calculations and the experimental dipole moment[23] are also listed in Table I. The Hartree–Fock and DFT calculations were carried out using the GAUSSIAN 98 program. The Hartree–Fock calculations of the momentum profiles were performed by using Eq. (3) with the basis sets of STO-3G, 6-31G, 6-311++G**, and aug-cc-pVTZ. The B3LYP functionals are used for the DFT calculations, respectively. Three basis sets of 6-31G, 6-311++G**, and aug-cc-pVTZ are used for the DFT calculations.

A. STO-3G

A minimal basis set, effectively of single ζ quality, use a single contraction of three Gaussian functions for each basis functions. Thus each function consists of C$(6s,3p)/[2s,1p]$, F$(6s,3p)/[2s,1p]$, and H$(3s)/[1s]$ contractions. Therefore, a total of 17 CGTO is employed for difluoromethane. This basis set was designed by Pople and co-workers.[24]

B. 6-31G

The 6-31G basis comprises an inner valence shell of six *s*-type Gaussians and an outer valence shell which has been split into two parts represented by three and one primitives. Both of carbon and fluorine atoms have a $(10s,4p)/[3s,2p]$ contraction and hydrogen atoms have a $(4s)/[2s]$ contraction. A total of 31 CGTO is used for difluoromethane. A detailed description of this basis set developed by Pople and the co-workers can be found in Ref. 25.

C. 6-311++G**

The 6-311++G** is an augmented version by Pople *et al*. The outer valence shell is split into three parts and represented by three, one and one primitives. Based on the 6-311G basis very diffused *s*- and *p*-functions are added to both of carbon and fluorine atoms and diffuse *s*-function are added to hydrogen atoms.[25–27] In addition, polarization functions are also included in the basis, a single set of five *d*-type Gaussian functions for F and C atoms and a single set of uncontracted *p*-type Gaussian functions for H atoms. Thus a $(12s,6p,1d)$ contracts to $[5s,4p,1d]$ for C and F atoms, and a $(6s,1p)$ to $[4s,1p]$ for H atoms. The number of CGTO is 80 for difluoromethane.

D. aug-cc-pVTZ

The augmented correlation consistent polarized valence triple ζ (cc-pVTZ) basis set (aug-cc-pVTZ) was taken from the work of Dunning *et al.*[28,29] The basic idea behind the correlation consistent basis sets is that functions which contribute approximately the same amount of correlation energy should be grouped together when considering what mixture of *s, p, d,* etc. basis functions to use. For hydrogen the polarization exponents were determined by optimizing them at the singly and doubly excited configuration interaction (SD-CI) level calculation for molecular hydrogen in its ground state. The (s,p) exponents for B-Ne were optimized in atomic Hartree–Fock calculations on the ground state. The polarization exponents were optimized at the SD-CI level. The extra diffuse nonpolarization functions were optimized in Hartree–Fock calculations on the lowest state of the anion. The extra polarization functions were optimized in SD-CI calculations. Both of carbon and fluorine atoms have a $(10s,5p,2d,1f)/[4s,3p,2d,1f]$ contraction and hydrogen atoms have a $(5s,2p,1d)/[3s,2p,1d]$ contraction. The number of CGTO is 118 for difluoromethane.

The optimized geometry of difluoromethane has been used for all the calculations. In order to compare the calculated cross sections with the experimental electron momentum profiles the effects of the finite spectrometer acceptance angles in both θ and ϕ ($\Delta\theta=\pm0.6°$ and $\Delta\phi=\pm1.2°$) were included using the Gaussian-weighted planar grid (GW-PG) method.[30]

III. EXPERIMENTAL METHODS

Details of the electron momentum spectrometer constructed at Tsinghua University have been reported.[31] Therefore only a brief description is given in this paper. Two hemispherical electron energy analyzers, each having a five element cylindrical retarding lens system, are mounted on two independent horizontal concentric turntables inside a μ-metal shielded vacuum system. In the present work, the polar angles of both analyzers are kept fixed at 45°. One analyzer turntable is kept in a fixed position while the other one is rotated to vary the relative azimuth angle. Each energy analyzer has a position sensitive detector consisting of two microchannel plates and a resistive anode in the energy dispersive exit plane. The energy range of each analyzer was set at 600 ± 4 eV with a pass energy of 50 eV. Electron impact ionization was carried out at an impact energy of 1200 eV plus the binding energy under the symmetric noncoplanar geometry. The energy resolution obtained in the coincidence experiment is a convolution of the two analyzer response functions and the energy distribution of the incident electron beam. It also depends on the deceleration ratio of the lens.

The coincidence energy resolution of the spectrometer was measured to be 1.15 eV full width at half maximum from the experiment on the argon $3p$ state. The experimental momentum resolution is estimated to be about 0.1 a.u. from a consideration of the argon $3p$ angular correlation. The sample of difluoromethane (99.0% purity) was used without further purification. No evidence of impurities was found in the binding energy spectra.

IV. RESULTS AND DISCUSSION

Difluoromethane (CH_2F_2) contains 26 electrons and has C_{2V} symmetry point group. The ground state electronic configuration can be written as

$$\underbrace{(\text{core})^6(3a_1)^2(2b_2)^2(4a_1)^2}_{\text{inner valence}}\underbrace{(5a_1)^2(3b_2)^2(1b_1)^2(1a_2)^2(6a_1)^2(4b_2)^2(2b_1)^2}_{\text{outer valence}}.$$

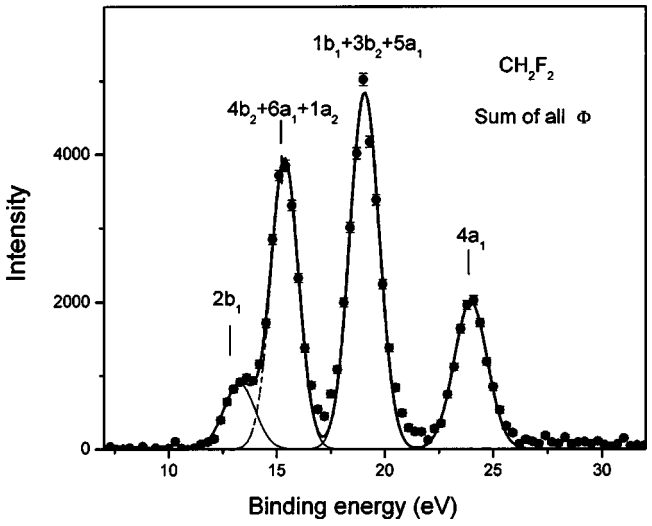

FIG. 1. Valence shell binding energy spectra of 1200 eV for difluoromethane at sum of all φ angles. The dashed and solid lines represent individual and summed Gaussian fits, respectively.

TABLE II. Ionization energies (eV) for difluoromethane.

	Experimental			Theoretical	
Orbital	EMS[a]	PES[b]	PES[c]	MS-$X\alpha$[d]	Hartree–Fock[e]
$2b_1$	13.3	13.3	13.17	14.92	14.79
$4b_2$		15.4	14.91	17.09	16.99
$6a_1$	15.4[f]	15.4	15.20	17.28	17.22
$1a_2$		15.8	15.61	18.20	18.12
$1b_1$		19.1	18.51	20.50	20.37
$3b_2$	19.1[g]	19.1	19.07	20.97	20.83
$5a_1$		19.1	19.76	21.23	21.08
$4a_1$	24.0	24.0	23.86	26.71	26.53
$2b_2$		38.2	38.20	43.62	43.44
$3a_1$		40.1	40.13	45.17	44.96

[a]Experimental EMS data in this work.
[b]Reference 19.
[c]Reference 20.
[d]Reference 29.
[e]Theoretical calculation of orbital energies with HF/aug-cc-pVTZ in this work.
[f]The peak of $4b_2$, $6a_1$, and $1a_2$ orbitals.
[g]The peak of $1b_1$, $3b_2$, and $5a_1$ orbitals.

The valence shell contains ten molecular orbitals and can be divided into two sets of three inner valence and seven outer valence orbitals. The order of these valence orbitals has been established both by PES and molecular calculations.[19]

A. Binding energy spectra

In order to obtain the experimental momentum profiles, 12 binding energy spectra over the energy range of 7–32 eV which cover seven outer valence orbitals and one inner valence orbital were collected at the out-of-plane azimuth angles φ=0°, 1°, 2°, 3°, 4°, 6°, 8°, 10°, 12°, 14°, 16°, and 21° in a series of sequential repetitive scans. The binding energy spectra of difluoromethane in the range 7–32 eV for measurements at the sum of all the φ angles is shown in Fig. 1 at the incident energy of 1200 eV plus the binding energy. The spectra in Fig. 1 are fitted with a set of individual Gaussian peaks. The fitted Gaussians for individual peaks are indicated by dashed lines while their sum, i.e., the overall fitted spectra, are represented by the solid lines. The widths of the peaks are combinations of the EMS instrumental energy resolution and the corresponding Franck–Condon widths derived from high resolution PES data.[19]

The PES spectrum of the seven outer valence and one inner valence region has been reported by Bieri, Åsbrink, and von Niessen.[19] In this work, the vertical ionization potentials of the $2b_1$, $4b_2$, $6a_1$, $1a_2$, $1b_1$, $3b_2$, $5a_1$, and $4a_1$ orbitals were determined to be 13.3, 15.4, 15.4, 15.8, 19.1, 19.1, 19.1, and 24.0 eV, respectively.

In the EMS binding energy spectra of Fig. 1, however, only four structures could be clearly identified. The ionization peak for the highest occupied molecular orbital (HOMO), $2b_1$ at 13.3 eV is well resolved. The next three outer valence orbitals with the 15.4 eV average vertical ionization potential, $4b_2$, $6a_1$, and $1a_2$, are not well separated experimentally due to their small energy separations.[19] The same is true of the next three outer valence orbitals with the 19.1 eV average vertical ionization potential, $1b_1$, $3b_2$, and $5a_1$, which even the high resolution PES could not resolve.[19] The band located at 24.0 eV corresponds to the ionization of the $4a_1$ orbital. A comparison of the valence shell binding energies of difluoromethane of this work and the experimental PES data[19,20] and the earlier published and our calculated theoretical values is given in Table II. It can be seen that the present measured EMS data are consistent with the previously published high resolution PES data. Some weak structures above 26 eV are observed which may due to correlation effects in the target or in the final state of residual ion.

Calculated binding energy spectra are compared with the measured binding energy spectra in Fig. 2. The synthesized theoretical spectra are obtained by summing the calculated densities over the same momentum range as the experiment, and using the calculated energy levels of the different orbitals. Both of the calculated density and energy levels of different orbitals come from the HF/aug-cc-pVTZ calculation. In comparing the experimental and theoretical binding en-

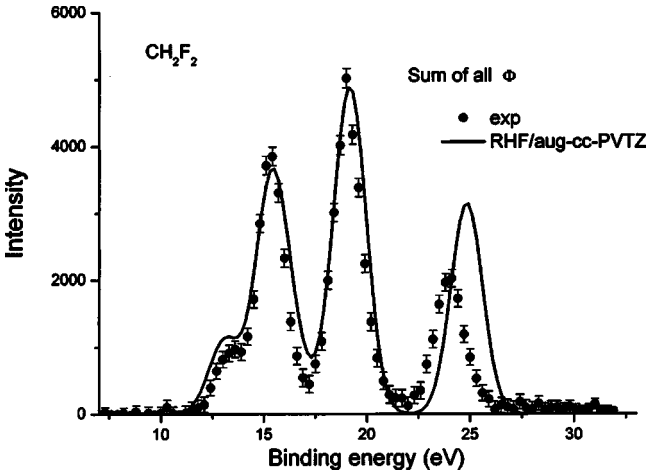

FIG. 2. Experimental and synthetic binding energy spectra of difluoromethane at sum of all φ angles. The solid curve is the Hartree–Fock calculation with aug-cc-pVTZ basis set. See text for details.

ergy spectra, it should be noted that the calculated energy levels has been shifted by 1.60 eV so that the energy of the $2b_1$ orbital agrees with the corresponding 13.17 eV peak in the experimental PES.[20] The measured EMS instrumental energy resolution function, as well as the widths of the transitions as observed in high resolution PES, have been folded into the calculated spectra. The experimental binding energy spectra are height normalized to the second peak of the calculated binding energy spectra.

It can be seen that the HF/aug-cc-pVTZ calculation is in reasonably good agreement with the experimental binding energy spectra for both relative energy position and intensity in the outer valence region. However, the calculation predicted significant splitting of ionization transitions from the $4a_1$ orbital due to strong electron correlation effects in the inner valence region. The predicted ionization energy level of $4a_1$ orbital is higher than the experiment and the calculation also overestimates the intensity of the ionization transition about 24 eV, which suggests that the theory should contain lower pole strength for the $4a_1$ orbital and this is also consistent with the comparison of the measured and calculated momentum profiles of the $4a_1$ orbital presented in the following section.

B. Experimental and theoretical momentum distributions

Experimental momentum profiles (XMPs) have been extracted by deconvolution of the sequentially obtained angular-correlated binding energy spectra, and therefore the relative normalization for the different transitions is maintained. For all the orbitals, the various theoretical momentum profiles (TMPs) are obtained with the methods described in Sec. II and the experimental instrumental angular resolutions have been incorporated in the calculations using the UBC RESFOLD program based on the GW-PG method.[30] Experimental data and theoretical values have been placed on a common intensity scale by normalizing the experimental to the DFT-B3LYP/6-311++G** theoretical momentum profile for the $2b_1$ orbital (see Fig. 3) and the relative normalization is preserved for all the other orbitals.

The theoretical and experimental momentum profiles of the outer valence orbitals and $4a_1$ inner valence orbital of difluoromethane are presented in Figs. 3–6. In the following discussion the comparisons between the theoretical calculations and the experimental data are provided for these orbitals.

The electron density of the HOMO plays an important role in determining the chemical reactivity as indicated by the frontier molecular orbital theory of Fukui[32] and the work of Woodward and Hoffman.[33] Therefore it is important to obtain a detailed understanding of the electronic structure of the HOMO. The currently determined experimental momentum profile for the $2b_1$ HOMO of CH_2F_2 is shown in Fig. 3, together with the theoretical momentum profiles calculated using HF and DFT/B3LYP methods employing the STO-3G, 6-31G, 6-311++G**, and aug-cc-pVTZ basis sets. This orbital has a ''*p*-type'' momentum distribution character as shown in Fig. 3. In the momentum range above 0.25 a.u., it can be seen that, except for HF/STO-3G, the calculated theoretical momentum profiles provide a good agreement with the experimental profile and the DFT-B3LYP with aug-cc-pVTZ calculation gives the best fit. Whereas, the small residual experimental intensity is in excess of all the calculations for the HOMO of difluoromethane in the momentum region below 0.25 a.u. The discrepancy between experiment and theory in the low momentum region is probably due to inaccuracies in the Gaussian fitting procedures since the nearby two ionization peaks, i.e., the first peak and the second peak in the binding energy spectra in Fig. 1 are close and the second peak, i.e., the $4b_2+6a_1+1a_2$ peak is large and could leak into the first peak in the low momentum range. Another possible source for the discrepancy in the low momentum range could be because of the distorted wave effects

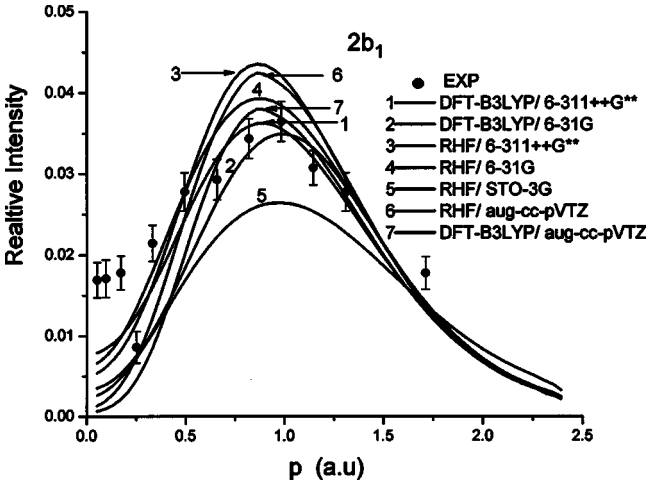

FIG. 3. Experimental and calculated momentum distributions for the HOMO $2b_1$ of difluoromethane. The TMPs are calculated by using Hartree–Fock method (curve 3, 4, 5, and 6) with the 6-311++G**, 6-31G, STO-3G, and aug-cc-pVTZ basis sets and DFT-B3LYP (curve 1, 2, and 7) method with the 6-311++G**, 6-31G, and aug-cc-pVTZ basis sets.

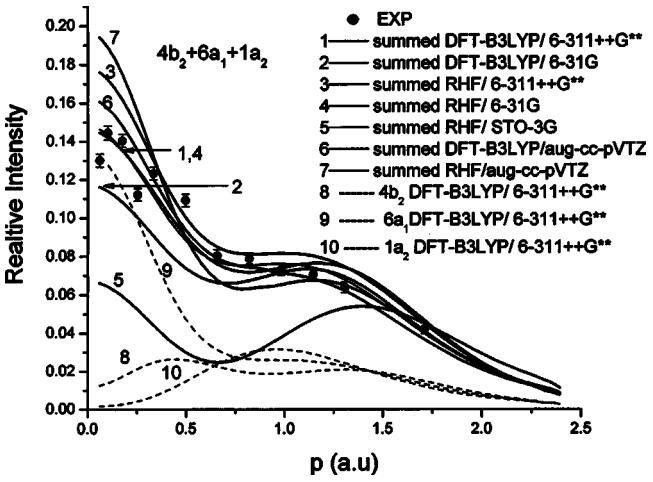

FIG. 4. Experimental and calculated spherically averaged momentum distributions for the summed and individual orbitals of the $4b_2$, $6a_1$, and $1a_2$ orbitals of difluoromethane. The TMPs are calculated by using Hartree–Fock method (curve 3, 4, 5, and 6) with the 6-311++G**, 6-31G, STO-3G, and aug-cc-pVTZ basis sets and DFT-B3LYP (curve 1, 2, and 7) method with the 6-311++G**, 6-31G, and aug-cc-pVTZ basis sets. The TMPs of individual orbitals are calculated by using the DFT-B3LYP method with the 6-311++G** basis set (curve 8, 9, and 10).

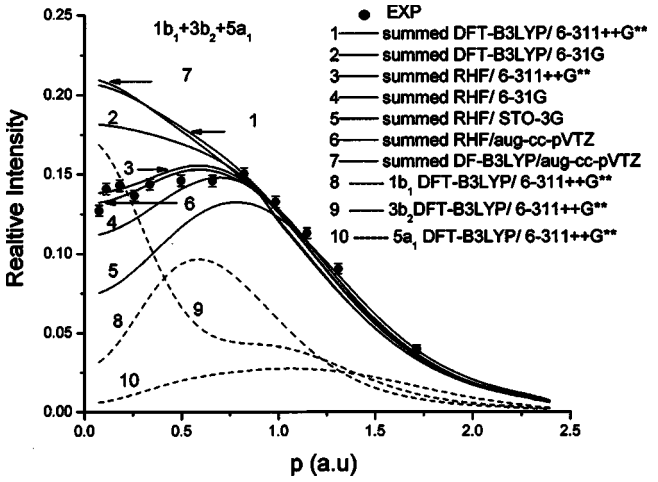

FIG. 5. Experimental and calculated spherically averaged momentum distributions for the summed and individual orbitals of the $1b_1$, $3b_2$, and $5a_1$ orbitals of difluoromethane. The TMPs are calculated by using Hartree–Fock method (curve 3, 4, 5, and 6) with the 6-311++G**, 6-31G, STO-3G, and aug-cc-pVTZ basis sets and DFT-B3LYP (curve 1, 2, and 7) method with the 6-311++G**, 6-31G, and aug-cc-pVTZ basis sets. The TMPs of individual orbitals are calculated by using the DFT-B3LYP method with the 6-311++G** basis set (curve 8, 9, and 10).

since the $2b_1$ orbital is a π^*-like molecular orbital, which is in agreement with Brundle, Robin, and Basch's conclusion that the orbital contains a large fraction C–F π antibonding character.[34] It has been found[35,36] that such orbitals usually produce a ''turn-up'' of the cross section in the low momentum range, and this behavior is similar to the low-p effect observed in atomic d-orbital XMPs. This situation is also probably the case for the $2b_1$ orbital of difluoromethane. Such effects in atoms have been attributed to distorted wave effects that increase the calculated cross sections at low p as observed in the experimental measurements.[32] Similar behavior has been seen in the XMPs of transition-metal hexacarbonyl HOMOs that are known to be largely metal nd in character.[37] The corresponding transition-metal atoms show such behavior and this is found to decrease with increase in impact energy[34] in the distorted wave impulse approximation (DWIA) calculations. Unfortunately at present DWIA calculations are possible only for atoms but not for molecules due to the multicenter nature of the latter. However, the discrepancy in the low momentum range could be because no calculation could reproduce the experimental momentum profile. Usually, HOMO orbitals are very diffuse in position space and thus their diffuse outer regions are likely difficult to be well modeled by the SCF and DFT variational calculations.

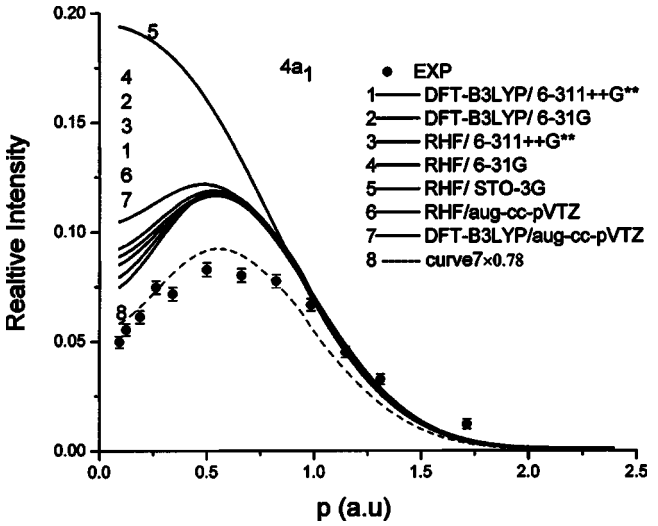

FIG. 6. Experimental and calculated spherically averaged momentum distributions for the inner valence orbital $4a_1$ of difluoromethane. The TMPs are calculated by using Hartree–Fock method (curve 3, 4, 5, and 6) with the 6-311++G**, 6-31G, STO-3G, and aug-cc-pVTZ basis sets and DFT-B3LYP (curve 1, 2, and 7) method with the 6-311++G**, 6-31G, and aug-cc-pVTZ basis sets. The curve 8 is due to the curve 7 multiplied by an estimated pole strength of 0.78.

The next three orbitals, $4b_2$, $6a_1$, and $1a_2$ are closely spaced and cannot be resolved due to the poor energy resolution of EMS. Only the summed experimental momentum profiles for the $(4b_2+6a_1+1a_2)$ orbitals are shown in Fig. 4, together with the theoretical momentum profiles calculated using HF and DFT-B3LYP methods with the STO-3G, 6-31G, 6-311++G**, and aug-cc-pVTZ basis sets. The $4b_2$ orbital has a ''p-p'' type character and $1a_2$ has a p-type distribution, while the $6a_1$ orbital which is dominant in the summed momentum distribution shows a ''s-p'' type distribution, as indicated in Fig. 4. The summed momentum profile is therefore an s-p type distribution. It can be seen from Fig. 4 that for the same basis sets HF calculations (curves 3, 4, 6) predict higher momentum intensity than DFT-B3LYP calculations (curves 1, 2, 7) and the HF calculation with the 6-31G basis set is similar with the DFT/B3LYP calculation with the 6-311++G** basis set. The DFT/B3LYP calculated theoretical momentum distribution with 6-311++G** basis sets and the HF/6-31G calculation reproduce the experimental momentum distribution in both shape and magnitude while the HF calculation with the STO-3G basis set severely underestimates the densities. It could be seen that it is hard to choose the different calculations, including the methods and the size of basis sets employed with the exception of the minimum level calculation of HF/STO-3G.

The third peak of difluoromethane corresponds to $1b_1$, $3b_2$, and $5a_1$ ionizations, which are also too close to be separately resolved. In Fig. 5, the summed experimental momentum distribution is shown together with the theoretical momentum distributions calculated using HF and DFT/B3LYP methods with various basis sets. In the momentum range above 1.0 a.u., it can be seen that all the calculated theoretical momentum profiles provide a good agreement with the experimental profile. It could also be seen that choosing different theoretical methods and basis sets both strongly affect the calculated momentum distribution of the summed momentum densities in the momentum region below 1.0 a.u. Thus, the experimental distribution acts as a criterion for evaluating the quality of quantum chemical calculations. Usually, a calculated electron momentum density of the corresponding Kohn–Sham DFT which includes electron correlation in theoretical calculations gives a better description of the measured momentum profile than the descriptions of canonical Hartree–Fock orbitals. However, the DFT-B3LYP calculations have a worse agreement with the

experimental profiles than the corresponding Hartree–Fock calculations and the HF calculation with the aug-cc-pVTZ basis set gives the best fit of the experimental result. Furthermore, the DFT-B3LYP calculation with the larger basis set, i.e., aug-cc-pVTZ basis set, has worse fit of the experimental profile than the smaller basis set, i.e., 6-31G basis set. Therefore, it is also shown that it is very hard to choose between the different calculations, including the methods and the size of basis sets.

Unlike these outer valence orbitals, the $4a_1$ inner valence orbital is clearly separated in the EMS binding energy spectra (see Fig. 1). The orbital has a *p*-type momentum distribution character as shown in Fig. 6 and it could also be seen that the theoretical results with various basis sets are similar in the momentum range above about 0.75 a.u. while the calculations with different methods and basis sets strongly affect the description of the momentum density in the low momentum region (diffuse large *r* region) which could be important for chemical reactivity and possibly molecular recognition.[38,39] The comparison between the experimental data and theoretical calculations in Fig. 6 shows that all the seven calculations significantly overestimate the experimental intensity. This indicates that some of the transition intensity from this orbital is located in the higher binding energy range due to the final state electron correlation effects and this has been discussed in the calculation of the synthesized theoretical binding energy spectra. In order to compare the shape of the momentum distribution the DFT-B3LYP/aug-cc-pVTZ calculation is multiplied by an estimated pole strength of 0.78 and the reproduced momentum profile is represented by curve 8 in Fig. 6. Then the experimental result is well described by the DFT-B3LYP/aug-cc-pVTZ calculation.

V. SUMMARY

In summary, the first measurements of the valence shell binding energy spectra and momentum distributions of all the outer valence and $4a_1$ inner valence orbital of CH_2F_2 by the electron momentum spectroscopy are reported. The experimental momentum distributions are compared with the theoretical momentum profiles calculated using HF and DFT/B3LYP methods employing the STO-3G, 6-31G, 6-311++G**, and aug-cc-pVTZ basis sets. The binding energies are in excellent agreement with previously published PES data and the synthesized theoretical spectra are compared with the experimental binding energy spectra, from which it can be seen that the HF/aug-cc-pVTZ calculation is in reasonably good agreement with the experimental binding energy spectra in the outer valence region while the calculation predicted significant splitting of ionization transitions from the $4a_1$ inner valence orbital due to strong electron correlation effects in the inner valence region. In comparing the experimental momentum profiles with the calculated distributions, although the experimental profiles could be generally well described by the calculations when large and diffuse basis sets are used, it also shows that it is hard to choose the different calculations for some orbitals, including the methods and the size of basis sets employed. The pole strength of the ionization peak from the $4a_1$ inner valence orbital is also estimated.

ACKNOWLEDGMENTS

The authors would like to acknowledge valuable discussions with Professor Zhu Qihe. Project supported by the National Natural Science Foundation of China under Grant Nos. 19854002, 19774037, and 10274040 and the Research Fund for the Doctoral Program of Higher Education under Grant No. 1999000327.

[1] I. E. McCarthy and E. Weigold, Rep. Prog. Phys. **91**, 789 (1991), and references therein.
[2] I. E. McCarthy and E. Weigold, Phys. Rep. **C27**, 275 (1976).
[3] C. E. Brion, Int. J. Quantum Chem. **29**, 1397 (1986).
[4] A. O. Bawagan, C. E. Brion, E. R. Davidson, and D. Feller, Chem. Phys. **113**, 4704 (1987).
[5] J. Rolke, Y. Zheng, C. E. Brion, Z. Shi, S. Wolfe, and E. R. Davidson, Chem. Phys. **244**, 1 (1999).
[6] L. Rolke and C. E. Brion, Chem. Phys. **207**, 173 (1996).
[7] P. Duffy, D. P. Chong, M. E. Casida, and D. R. Salahub, Phys. Rev. A **50**, 4704 (1994).
[8] P. Duffy, Can. J. Phys. **74**, 763 (1996).
[9] Y. Zheng, J. J. Neville, and C. E. Brion, Science **270**, 5237 (1995).
[10] D. A. Winkler, M. T. Michalewiez, F. Wangr, and M. J. Brunger, J. Phys. B **32**, 3239 (1999).
[11] J. K. Deng, G. Q. Li, X. D. Wang, J. D. Huang, H. Deng, C. G. Ning, and Y. Wang, J. Chem. Phys. **117**, 4839 (2002).
[12] J. K. Deng, G. Q. Li, F. Wang, G. L. Su, C. G. Ning, T. Zhang, X. G. Ren, and Y. Wang, J. Chem. Phys. **120**, 10009 (2004).
[13] Neerja, A. N. Tripathi, and V. H. Smith, Jr., J. Phys. B **34**, 1233 (2001).
[14] M. E. Casida, Phys. Rev. A **51**, 2005 (1995).
[15] D. L. Copper, K. A. Mort, N. L. Allan, D. Kinchington, and C. Mcguigan, J. Am. Chem. Soc. **115**, 12615 (1993).
[16] C. Womeldorf and W. Grosshandler, Combust. Flame **118**, 25 (1999).
[17] M. K. Ellis, R. Trebilcock, J. L. Naylor, K. Tseung, M. A. Collins, P. M. Hext, and T. Green, Fundam. Appl. Toxicol. **31**, 243 (1996).
[18] B. P. Pullen, T. A. Carlson, W. E. Moddeman *et al.*, J. Chem. Phys. **53**, 768 (1970).
[19] G. Bieri, L. Åsbrink, and W. Von Niessen, J. Electron Spectrosc. Relat. Phenom. **23**, 281 (1981).
[20] M. S. Banna and D. A. Shirley, Chem. Phys. Lett. **33**, 441 (1975).
[21] M. Speis, U. Delfs, and K. Lucas, Fluid Phase Equilib. **170**, 285 (2000).
[22] G. L. Su, C. G. Ning, S. F. Zhang *et al.*, Chem. Phys. Lett. **390**, 162 (2004).
[23] E. W. Lemmon, M. O. McLinden, and M. L. Huber, *NIST Reference Fluid Thermodynamic and Transport Properties (REFPROP), Version 7.1* (National Institute of Standards and Technology, Boulder, CO, 2003).
[24] W. J. Hehre, R. F. Stewart, and J. A. Pople, J. Chem. Phys. **51**, 2657 (1969).
[25] R. Krishnan, M. J. Frisch, and J. A. Pople, J. Chem. Phys. **72**, 4244 (1980).
[26] T. Clark, J. Chandrasekhar, G. W. Spitznagel, and P. V. R. Schleyer, J. Comput. Chem. **4**, 294 (1983).
[27] M. J. Frisch, J. A. Pople, and J. S. Binkley, J. Chem. Phys. **80**, 3265 (1984).
[28] T. H. Dunning, Jr., J. Chem. Phys. **90**, 1007 (1989).
[29] D. E. Woon and T. H. Dunning, Jr., J. Chem. Phys. **98**, 1358 (1993).
[30] P. Duffy, M. E. Casida, C. E. Brion, and D. P. Chong, Chem. Phys. **159**, 347 (1992).
[31] J. K. Deng, G. Q. Li, Y. He *et al.*, J. Chem. Phys. **114**, 882 (2001).
[32] K. Fukui, Acc. Chem. Res. **4**, 157 (1971).
[33] R. B. Woodward and R. Hoffman, *The Conservation of Orbital Symmetry* (Verlag Chemie, Weinheim, 1970).
[34] C. R. Brundle, M. B. Robin, and H. Basch, J. Chem. Phys. **53**, 2196 (1970).

[35] C. E. Brion, Y. Zheng, J. Rokle, J. J. Neville, I. E. McCarthy, and J. Wang, J. Phys. B **31**, L223 (1998).
[36] J. Rolke, Y. Zheng, C. E. Brion, Z. Shi, S. Wolfe, and E. R. Davidson, Chem. Phys. **244**, 1 (1999).
[37] J. Rolke, Y. Zheng, C. E. Brion, S. J. Chakravorty, E. R. Davidson, and I. E. McCarthy, Chem. Phys. **215**, 191 (1997).
[38] C. E. Brion, G. Cooper, Y. Zheng *et al.*, Chem. Phys. **270**, 13 (2001).
[39] K. Fukui, Angew. Chem., Int. Ed. Engl. **21**, 801 (1982).